

# Optical velocity meter based on Ramsey oscillations in a double-grating setup

J. Preclíková,<sup>1</sup> M. Kozák,<sup>2</sup> D. Fregenal,<sup>3</sup> and J. P. Hansen<sup>1</sup>

<sup>1</sup>*Department of Physics and Technology, University of Bergen, N-5007 Bergen, Norway*

<sup>2</sup>*Faculty of Mathematics and Physics, Charles University in Prague, Ke Karlovu 3, 121 16 Prague 2, Czech Republic*

<sup>3</sup>*Centro Atómico Bariloche and Consejo Nacional de Investigaciones Científicas y Técnicas. R8402AGP S.C. de Bariloche, Argentina*

(Received 13 November 2013; published 7 April 2014)

We propose a method for measuring velocities of atoms or molecules in a gas phase based on time-resolved laser experiments. Two intensity gratings of electromagnetic field with variable time delay  $\tau$  are created by interfering of four laser pulses. Using first-order perturbation theory, we show that such arrangement can be used for measuring particle velocities, which have an optical transition to a long-living excited state. It is shown that the optical Ramsey oscillations obtain a characteristic modulation that reflects the distribution of velocities.

DOI: [10.1103/PhysRevA.89.043406](https://doi.org/10.1103/PhysRevA.89.043406)

PACS number(s): 32.80.Rm, 32.80.Wr, 06.30.Gv

## I. INTRODUCTION

Precise characterization of particle velocities in beams is crucial for minimizing the uncertainty in measurements of fundamental physical quantities and in basic chemistry, e.g., in determination of polarizabilities, dipole moments, in reactivity studies, and in deflection experiments [1]. The most common methods for determining the particle velocities in gas phase are Doppler velocimetry [2], time-of-flight (TOF) method [3], laser-induced fluorescence [4], and determining of the Doppler shift in absorption lines [5]. However, to reach a high accuracy in velocity measurements is still a challenging task. Several methods with accuracy better than 1% have been developed: mechanical velocity selectors [6], TOF with extraordinary precise measurements of the arrival time distribution of particles [7], atom interferometry on nanogratings [8], and devoted nanogratings-based phase choppers [9].

Few optical methods for velocity measurements based on the interaction of a gas with light intensity gratings were implemented. The main advantage of the optical methods is that they are nonintrusive and can offer the spatial information about the velocity distribution. On the other hand, these methods are based on coherent effect such as photon echo [10] or on nonlinear effects such as four-wave mixing [11], coherent anti-Stokes Raman scattering [12], or on creating a thermal grating [13] or on photothermal deflection [14], so high laser intensities are required.

Usage of standard Ramsey interferometry [15,16] for characterizing velocities in an atomic fountain is described in [17]; the transient times (velocities) are extracted indirectly from the Fourier transform of the Ramsey signal measured as a function of precisely varied frequency.

In this work, we propose a method based on observation of time modulation of amplitudes of optical Ramsey fringes. We suggest direct measurement of Ramsey fringes as a function of time between two incident intensity gratings created by interference of four ultrashort laser pulses. Our method can offer interferometric accuracy, depending on how the time delay between the pulses can be controlled.

Optical Ramsey fringes in time-resolved pump and probe experiments are observed as fast oscillations of the population of excited states, which varies as  $\cos(\omega_{lg}\tau)$ , where  $\omega_{lg}$  is frequency of transition between ground  $g$  and excited  $l$  states and  $\tau$  is the time delay between the pump and probe pulses,

which need to be phase locked [18–21]. Our method is based on introducing pump and probe gratings, which are created at the crossing of two laser beams (see Fig. 1). Each laser beam contains a pair of laser pulses with precisely controllable time delay  $\tau$ . The first pulses create a pump grating with spatial intensity profile due to interference, while the second pulses create probe grating. If we introduce an atomic (molecular) beam in the  $x$  direction, its velocity can be monitored by changes in the modulation of the amplitude of the Ramsey fringes oscillations as the function of the time delay between the pump and probe gratings.

The method can be applied to any system that has a long-living excited level which can be coupled to the ground state by the laser. Suitable systems can be, for example, a dilute gas of atoms and the laser transition can be to Rydberg levels with subsequent detection by selective field ionization [22–25], or molecular systems with state detection by laser-induced fluorescence, or by photoionization [26,27]. We estimate that the accuracy of the determination of the mean velocity can be very precise and the width of the velocity distribution can be determined from the expected signal as well.

## II. THEORY

The electromagnetic field created by the interference of two Gaussian laser pulses, which cross under angle  $\theta$ , can be described by the following vectors:

$$\begin{aligned}\vec{E}_1(\vec{r}, t) &= E_0 e^{-\alpha t^2} \cos(\omega t - \vec{k}_1 \cdot \vec{r}) \vec{e}_z, \\ \vec{E}_2(\vec{r}, t) &= E_0 e^{-\alpha t^2} \cos(\omega t - \vec{k}_2 \cdot \vec{r}) \vec{e}_z.\end{aligned}\quad (1)$$

with wave numbers defined as

$$\begin{aligned}\vec{k}_1 &= -k_x \vec{e}_x + k_y \vec{e}_y = \frac{2\pi}{\lambda} \left[ -\sin\left(\frac{\theta}{2}\right) \vec{e}_x + \cos\left(\frac{\theta}{2}\right) \vec{e}_y \right], \\ \vec{k}_2 &= k_x \vec{e}_x + k_y \vec{e}_y = \frac{2\pi}{\lambda} \left[ \sin\left(\frac{\theta}{2}\right) \vec{e}_x + \cos\left(\frac{\theta}{2}\right) \vec{e}_y \right].\end{aligned}\quad (2)$$

$E_0$  is the amplitude of the field,  $\alpha$  is the parameter that determines the laser pulse duration, and  $\omega$  is the laser frequency corresponding to the wavelength  $\lambda$ . The first crossed pulses result in creation of the following field profile:

$$\vec{E}_{G1}(t) = \vec{E}_1 + \vec{E}_2 = 2E_0 e^{-\alpha t^2} \cos(\omega t - k_y y) \cos(k_x x) \vec{e}_z.\quad (3)$$

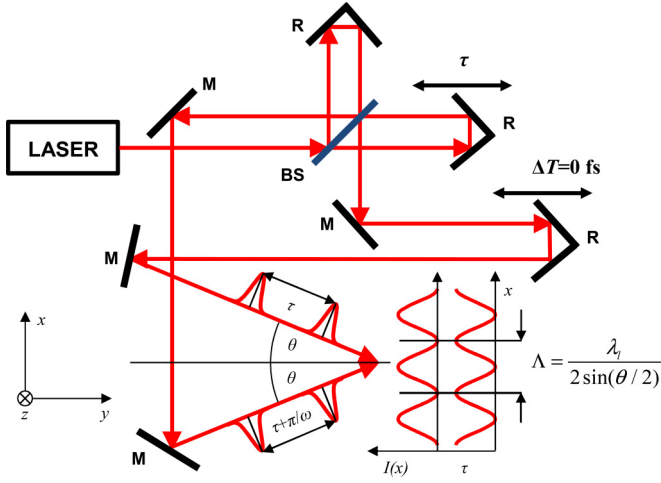


FIG. 1. (Color online) Scheme of the setup proposed for the double-grating experiment. The core of the experiment is variation of the Michelson interferometer, which is commonly used in the femto-second interferometry. R stands for retroreflector, M for mirror, and BS for beam splitter. After the BS, there are two outgoing beams, and each of them contains a pair of pulses with controllable delays  $\tau$ , resp.  $\tau + \pi/\omega$  (the phase shift is caused by the fact that the beam, which comes out in the direction towards laser, is reflected once more than the second beam). The delay between pulse pairs coming from the different arms of the interferometer can be precisely set to  $\Delta T = 0$  by changing the length of the optical path by using a transitional stage. The beams cross under angle  $\theta$  and create two intensity gratings: pump grating and probe grating at time  $\tau$ . Due to the phase shift  $\pi/\omega$ , the second (probe) grating is space shifted. The velocity component along the  $x$  direction can be monitored by this setup.

The spatial dependence of the envelope Gaussian function is neglected. This approximation is valid for pulses which are spatially longer than the characteristic dimensions of the investigated region. Regarding the setup proposed in Fig. 1, we see that the pulses in the second pair, which create the probe grating, are phase shifted by  $\pi$  due to the different number of reflections in the Michelson interferometer. The field of the probe grating  $\vec{E}_{G2}(t - \tau)$  is then described by

$$\vec{E}_{G2}(t - \tau) = E_0 e^{-\alpha(t-\tau)^2} \sin[\omega(t - \tau) - k_y y] \sin k_x x \vec{e}_z. \quad (4)$$

The grating constant  $\Lambda = \lambda/(2 \sin \theta/2)$  is identical for both field profiles  $\vec{E}_{G1}$  and  $\vec{E}_{G2}$ .

In the next step, we consider an atom moving linearly in the  $x$  direction with velocity  $v$  and position  $x(t) = x_0 + vt$ . If we introduce the dipole approximation, when the electric field at the position of an atomic core or a center of mass of a molecule can be considered to be the same for the whole electronic wave function and when the particle travels a distance  $x(t) < \Lambda$  during the duration of the laser pulse, the Hamiltonian can be described as

$$\hat{H} = \hat{H}_0 + \hat{W}(t, x(t)), \quad (5)$$

$$\hat{W}(t, x(t)) = e_0 \vec{r} \cdot \{\vec{E}_{G1}(t, x(0)) + \vec{E}_{G2}(t - \tau, x(\tau))\}, \quad (6)$$

where  $\hat{W}(t, x(t))$  is the perturbation,  $e_0$  is the charge of electron.

Within first-order time-dependent perturbation theory, the probability amplitude of an excited level  $l$ , coupled from the ground state  $g$  by the laser field of Eq. (5), can be written as

$$a_l(t) = -\frac{i}{\hbar} \int_{-\infty}^{\infty} \int \psi_l^* \hat{W}(t) \psi_g e^{i\omega_l t} d\vec{r} dt, \quad (7)$$

$$\text{where } \omega_l = \frac{1}{\hbar} (E_l - E_g). \quad (8)$$

Introducing dipole coupling element  $\Omega_{lg}$ ,

$$\Omega_{lg} = \int e_0 \psi_l^{*(0)} \vec{r} \psi_g^0 d\vec{r}, \quad (9)$$

and taking into account that the trigonometric functions  $\cos k_x x_0$ ,  $\sin k_x(x_0 + v\tau)$ ,  $\cos(\omega t - k_y y)$ ,  $\sin[\omega(t - \tau) - k_y y]$  only slightly vary over the region contributing to the integral of Eq. (9), the amplitude can be written as

$$\begin{aligned} a_l(\tau) &\cong -\frac{i}{\hbar} E_0 \Omega_{lg} \int_{-\infty}^{\infty} \{e^{-\alpha t^2} \cos(\omega t - k_y y) \cos k_x x_0 \\ &\quad - e^{-\alpha(t-\tau)^2} \sin[\omega(t - \tau) - k_y y] \\ &\quad \times \sin k_x(x_0 + v\tau)\} e^{i\omega_l t} dt \\ &\cong -\frac{i}{\hbar} E_0 \Omega_{lg} \sqrt{\frac{\pi}{\alpha}} e^{ik_y y} e^{-\frac{(\omega_l - \omega)^2}{4\alpha}} \\ &\quad \times [\cos k_x x_0 - i \sin k_x(x_0 + v\tau)] e^{i\omega_l \tau}, \end{aligned} \quad (10)$$

and the probability of excitation as

$$\begin{aligned} P(\tau, x_0, v) &= \frac{\pi}{\hbar^2 \alpha} \Omega_{lg}^2 E_0^2 e^{-\frac{(\omega_l - \omega)^2}{2\alpha}} \\ &\quad \times [\cos^2 k_x x_0 + \sin^2 k_x(x_0 + v\tau) \\ &\quad - 2 \cos k_x x_0 \sin k_x(x_0 + v\tau) \sin \omega_l \tau]. \end{aligned} \quad (11)$$

This expression describes the probability of excitation of a single particle with starting position  $x_0$ , moving with velocity  $v$  as a function of the time delay between pump and probe gratings  $\tau$ . In the next section, we will discuss its variation for cases of ensembles of particles with heterogeneous velocities.

### III. APPLICATIONS

#### A. Beam with Gaussian velocity distribution

In order to study the effect on the Ramsey fringes pattern of a given velocity distribution, we chose, as a first step, a Gaussian distribution with the following parameters: a mean velocity  $v_0$ , a width of distribution parameter  $\sigma$ , and a proportional constant  $K$ :

$$f(v) = K e^{-\frac{(v-v_0)^2}{2\sigma^2}}. \quad (12)$$

Then, the total probability of excitation is given by the solution of

$$P^{\text{all}}(\tau, x_0) = \int_{-\infty}^{\infty} f(v) P(\tau, x_0, v) dv, \quad (13)$$

which equals

$$P^{\text{all}}(\tau, x_0) = \frac{\pi}{\hbar^2 \alpha} \Omega_{lg}^2 E_0^2 K \sqrt{2\pi} \sigma e^{-\frac{(\omega_{lg} - \omega)^2}{2\alpha}} \left[ \frac{1}{2} + \cos^2 k_x x_0 - \frac{1}{2} e^{-2(\sigma k_x \tau)^2} \cos 2k_x (x_0 + v_0 \tau) - 2e^{-\frac{(\sigma k_x \tau)^2}{2}} \times \cos k_x x_0 \sin \omega_{lg} \tau \sin k_x (x_0 + v_0 \tau) \right]. \quad (14)$$

This function is plotted in the upper part of Fig. 2 for the case  $\theta = 20^\circ$ ,  $\lambda = 830$  nm,  $\omega_{lg}$  is fully resonant with  $\lambda$ ,  $\alpha = 10^{26}$  s $^{-2}$  corresponds to 150-fs-long pulse,  $K = 1$ ,  $\sigma = 100$  ms $^{-1}$ ,  $v_0 = 1000$  ms $^{-1}$ .

In the common pump and probe Ramsey interferometry, the population of the excited state oscillates as  $(1 + \cos \omega_{lg} \tau)$  [24]. Interferometry using intensity gratings and the movement of particles add new phenomena.

We first consider the effect of the spatial gratings. For static particles ( $v_0 = 0$ ), we would get the oscillating term  $(1 - \sin 2k_x x_0 \sin \omega_{lg} \tau)$  from Eq. (11). The term  $\sin \omega_{lg} \tau$  describes the Ramsey oscillations and it is completely analogous to  $\cos \omega_{lg} \tau$  from common Ramsey interferometry. The change of the harmonic function type is caused by the phase shift due to the different number of reflections in the interferometer arms. The modulation given by the term  $\sin 2k_x x_0$  reflects the more and the less effective spatial regions of  $x_0$ , where atoms are excited. It oscillates with a period which is half of the pump and probe grating period and the maxima positions correspond to regions where pump and probe gratings have the same intensity.

Secondly, the effect of atomic motion becomes interesting when the term  $v_0 \tau$  reaches the value of the grating constant  $\Lambda$ . For thermal velocities, it happens for  $\tau$  in the order of hundreds of ps or several ns. As the final state of a moving atom depends on starting position  $x_0$ , atom velocity  $v$ , and pump-probe delay  $\tau$ , an atom with its initial position in the maximum of the pump grating will be excited with much higher probability than the atoms located in the grating minima. The deexcitation probability of the moving excited atom depends not only on the time delay  $\tau$ , but also on its position, when the probe grating is applied. On the other hand, the atoms, which were not excited by the pump grating, can be excited by the probe grating, if they are in a right place.

Thirdly, the width of distribution  $\sigma$  of velocities contributes to the exponential damping of the Ramsey oscillations. The wider the distribution, the faster the damping.

Common detector systems do not have micrometer spatial resolution for particle detection. For instance, in the selective field ionization technique, the characteristic dimensions of the cone determining the resolution volume are on the order of few mm. The measured signal then corresponds to the integration over the broad region  $(-X, X)$  of  $x_0$  and terms oscillating with  $x_0$  are averaged to zero:

$$\text{Signal}(\tau, v) \propto \int_{-X}^X P(\tau, x_0) dx_0 \propto \left( 1 - e^{-\frac{(\sigma k_x \tau)^2}{2}} \sin k_x v_0 \tau \sin \omega_{lg} \tau \right). \quad (15)$$

The simulated signal is displayed in the lower panel of Fig. 2. It shows fast Ramsey oscillations,  $\sin \omega_{lg} \tau$ , with slower

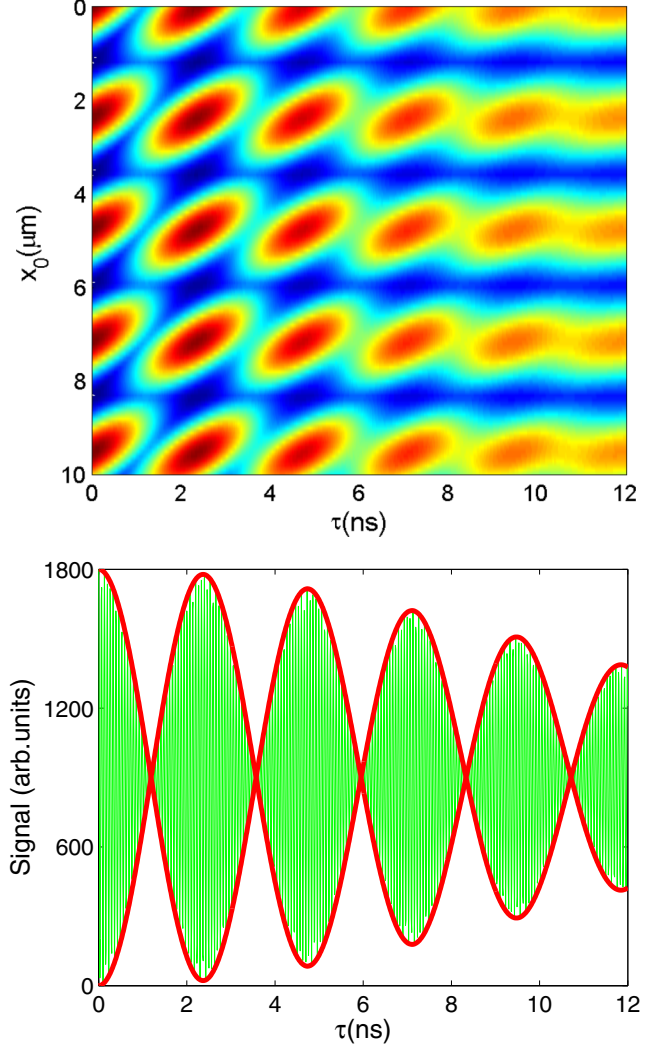


FIG. 2. (Color online) Upper panel: Map of amplitudes of Ramsey fringes oscillations as function of time delay between gratings  $\tau$  and position  $x_0$ . The Gaussian distribution of velocities [Eq. (12)] was considered. It shows results of function (14) with parameters  $\theta = 20^\circ$ ,  $\alpha = 10^{26}$  s $^{-2}$ ,  $K = 1$ ,  $\sigma = 100$  ms $^{-1}$ ,  $v_0 = 1000$  ms $^{-1}$ . The dark red color corresponds to the regions where the Ramsey fringes have the highest amplitudes. The tilt of the regions is caused by the interplay between the atom movement and the arriving of the probe grating. The smearing of the signal for longer  $\tau$  is caused by the fact that atoms have different velocities: the broader the distribution, the faster the smearing. Lower panel: Expected signal (corresponding to number of atoms in the excited level) according to Eq. (15). The red thick curves are signal envelopes. The inner oscillations are the result of sampling frequency, the real oscillations are faster with frequency  $\omega_{lg}$ .

modulation given by the term  $\sin k_x v_0 \tau$ . From this modulation, the mean velocity  $v_0$  of particles can be deduced. The other two variables in this term are precisely controlled in the experiment:  $\tau$  via delay line in the interferometer and  $k_x$  by the angle between the crossing beams  $\theta$ .

The mean velocity can be determined from the position of the signal nodes, when

$$k_x v \tau = N\pi, \quad N = 1, 2, 3 \dots \quad (16)$$

and the width of distribution from the damping of the signal.

**B. Thermal beam**

In the next step, we consider Ramsey fringes signal for a thermal beam with broad velocity distribution corresponding to a beam that is created from evaporating metal heated up to the temperature  $T$  in an oven with a narrow long output channel. We approximate the velocity distribution in the  $x$  direction by

$$f(v) = \sqrt{\left(\frac{m}{2\pi kT}\right)^3} 4\pi v^2 e^{-\frac{mv^2}{2kT}}, \quad (17)$$

where  $m$  is the mass of an atom or molecule and  $k$  is the Boltzmann constant.

In Fig. 3, the thermal velocity distribution [Eq. (17)] and the corresponding probability signal are shown for lithium atoms at 600 K. Notice that expected oscillations in the signal are damped quite quickly, but the first node is still apparent.

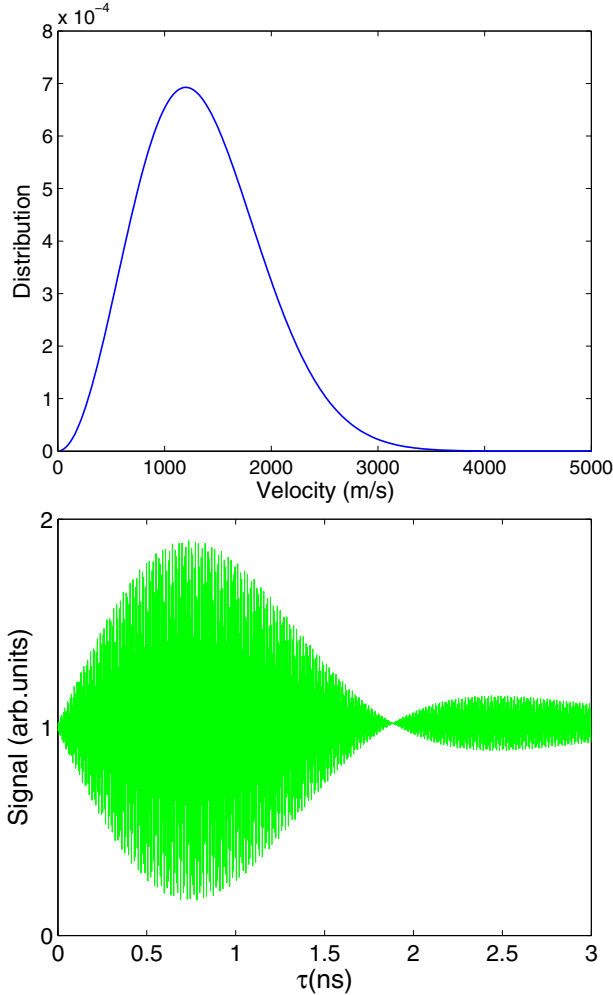


FIG. 3. (Color online) Upper panel: Thermal distribution of velocities of lithium atoms for  $T = 600$  K according to Eq. (17). Lower panel: Signal that will be detected in the case of velocity distribution displayed in the upper panel. The crossing angle  $\theta = 20^\circ$  and laser pulse parameter  $\alpha = 10^{26} \text{ s}^{-2}$ . The oscillations are a result of sampling frequency; the real inner oscillations are faster with frequency  $\omega_g$ .

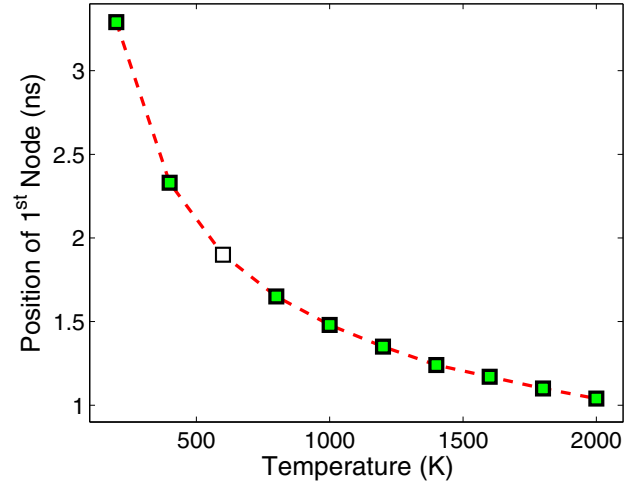


FIG. 4. (Color online) The expected position of the first node in the signal of Ramsey fringes as a function of temperature, when considering the thermal distribution of velocities given by Eq. (17). The white square corresponds to the node from Fig. 3.

The position of the first node is strongly dependent on the temperature of the particles (see Fig. 4). The position of the node, which was read from the signal in the lower part of Fig. 3, is highlighted by the white color. The phenomenon of the strong shift of the signal nodes with a particle main velocity can be used in a realization of an optical thermometer.

The double-transient-grating method can have a potential for characterizing of motion of cold atoms and molecules as well. It can represent an alternative to current optical methods for velocimetry of cold particles such as transient four-wave mixing [28], Bragg diffraction [29], velocimetry by electromagnetically induced transparency [30], or by recoil-induced resonances [31]. The main advantage of the double-transient-grating method is that it is very local and it can precisely address specific states in dependence on a selected wavelength. Supposing a mean velocity in one direction  $v_x = \sqrt{kT/2m}$  and using Eq. (16), we can estimate the occurrence time  $\tau$  of the first node as a function of the temperature

$$\tau = \frac{\pi}{k_x} \sqrt{\frac{m}{k}} \frac{1}{\sqrt{T}}. \quad (18)$$

It means that for measuring of velocity of particles with temperature down to several tens of  $\mu\text{K}$ , we need a lifetime of an excited state in the order of tens of  $\mu\text{s}$ , and such long lifetimes are characteristic for Rydberg states [32]. However, in the case of high excited Rydberg states, a short laser pulse addresses many of them due to their energy spacing that decreases as  $1/n^3$ , so typically a superposition of states is excited. Nevertheless, the superposition can be untangled by selective field ionization, where Ramsey oscillations only of a single level can be monitored.

In closing, the double-transient-grating method can offer very high accuracy since all of the key experimental variables, wavelength  $\lambda$ , crossing angle  $\theta$ , and time delay  $\tau$ , can be controlled with very high precision. The current state of the control of the time delay is on the subfemtosecond level [22].

The last crucial parameter is the clarity of the Ramsey fringes, which will depend on the selected detection method and successful suppression of the noise signal.

#### IV. CONCLUSIONS

In the presented work, we have proposed an experimental scheme for double-transient-grating experiment, which can serve as a velocity meter for particles in a gas phase. We

determined the evolution of Ramsey fringes for an ensemble of particles with Gaussian velocity distribution and with thermal distribution. We showed that the modulation of the Ramsey fringes envelope strongly reflected the main velocity in the system and the width of the distribution. We believe that this method can be directly applied for characterizing of velocity distribution of particle beams, and in the case of particles with accessible long-living excited state it will also display the temperature of a cold quantum gas.

- 
- [1] W. Christen, *J. Chem. Phys.* **139**, 024202 (2013).
- [2] J. W. Foreman, Jr., E. W. George, J. L. Jetton, R. D. Lewis, J. R. Thornton, and H. J. Watson, *IEEE J. Quantum Electron.* **2**, 260 (1966).
- [3] I. L. Kofsky and H. Levinstein, *Phys. Rev.* **74**, 500 (1948).
- [4] T. D. Gaily, S. D. Rosner, and R. A. Holt, *Rev. Sci. Instrum.* **47**, 143 (1976).
- [5] D. F. Davidson, A. Y. Chang, M. D. Di Rosa, and R. K. Hanson, *Appl. Opt.* **30**, 2598 (1991).
- [6] G. Tikhonov, V. Kasperovich, and V. V. Kresin, *Rev. Sci. Instrum.* **73**, 1204 (2002).
- [7] W. Christen, T. Krause, B. Kobin, and K. Rademan, *J. Phys. Chem. A* **115**, 6997 (2011).
- [8] W. F. Holmgren, M. C. Revelle, V. P. A. Lonij, and A. D. Cronin, *Phys. Rev. A* **81**, 053607 (2010).
- [9] W. F. Holmgren, I. Hromada, C. E. Klauss, and A. D. Cronin, *New J. Phys.* **13**, 115007 (2011).
- [10] M. Defour, J. C. Keller, and J. L. Le Gouet, *J. Opt. Soc. Am. B* **3**, 544 (1986).
- [11] R. B. Williams, P. Ewart, and A. Dreizler, *Opt. Lett.* **19**, 1486 (1994).
- [12] M. Lefebvre and M. Péalat, *J. Stremmel Opt. Lett.* **17**, 1806 (1992).
- [13] D. J. W. Walker, R. B. Williams, and P. Ewart, *Opt. Lett.* **23**, 1316 (1998).
- [14] J. A. Sell, *Appl. Opt.* **24**, 3725 (1985).
- [15] M. Hochstrasser, *Nature (London)* **268**, 17 (1977).
- [16] M. M. Salour and C. Cohen-Tannoudji, *Phys. Rev. Lett.* **38**, 757 (1977).
- [17] G. Di Domenico, L. Devenoges, A. Stefanov, A. Joyet, and P. Thomann, *Eur. Phys. J. Appl. Phys.* **56**, 11001 (2011).
- [18] N. F. Scherer, R. J. Carlson, A. Matro, M. Du, A. J. Ruggiero, V. Romero-Rochin, J. A. Cina, G. R. Flemming, and S. A. Ricai, *J. Chem. Phys.* **95**, 1487 (1991).
- [19] L. D. Noordam, D. I. Duncan, and T. F. Gallagher, *Phys. Rev. A* **45**, 4734 (1992).
- [20] J. F. Christian, B. Broers, J. H. Hoogenraad, W. J. van der Zalde, and L. D. Noordam, *Opt. Commun.* **103**, 79 (1993).
- [21] I. Liontos, C. Corsi, S. Cavalieri, M. Bellini, and R. Eramo, *Opt. Lett.* **36**, 2047 (2011).
- [22] R. R. Jones, C. S. Raman, D. W. Schumacher, and P. H. Bucksbaum, *Phys. Rev. Lett.* **71**, 2575 (1993).
- [23] M. Kozak, J. Preclikova, D. Fregenal, and J. P. Hansen, *Phys. Rev. A* **87**, 043421 (2013).
- [24] J. Preclikova, M. Kozak, D. Fregenal, O. Frette, B. Hamre, B. T. Hjertaker, J. P. Hansen, and L. Kocbach, *Phys. Rev. A* **86**, 063418 (2012).
- [25] R. E. Carley, E. D. Boleat, R. S. Minns, R. Patel, and H. H. Fielding, *J. Phys. B: At., Mol. Opt. Phys.* **38**, 1907 (2005).
- [26] V. Blanchet, M. A. Bouchene, and B. Girard, *J. Chem. Phys.* **108**, 4862 (1998).
- [27] H. Katsuki, K. Hosaka, H. Chiba, and K. Ohmori, *Phys. Rev. A* **76**, 013403 (2007).
- [28] M. Mitsunga, M. Yamashita, M. Koashi, and N. Imoto, *Opt. Lett.* **23**, 840 (1998).
- [29] J. W. R. Tabosa, A. Lezama, and G. C. Cardoso, *Opt. Commun.* **165**, 59 (1999).
- [30] F. B. M. Dos Santos and J. W. R. Tabosa, *Phys. Rev. A* **73**, 023422 (2006).
- [31] G. Di Domenico, G. Mileti, and P. Thomann, *Phys. Rev. A* **64**, 043408 (2001).
- [32] C. E. Theodosiou, *Phys. Rev. A* **30**, 2881 (1984).